Chirality

Symmetry Breaking in the Self-Assembly of Partially Fluorinated Benzene-1,3,5-tricarboxamides**

Patrick J. M. Stals, Peter A. Korevaar, Martijn A. J. Gillissen, Tom F. A. de Greef,
Carel F. C. Fitié, Rint P. Sijbesma,* Anja R. A. Palmans,* and E. W. Meijer*

In the early 1970s Young and co-workers described—hidden in a report on stilbene derivates forming nematic liquid crystals—a fascinating phenomenon: the formation of optically active phases out of racemic or achiral mixtures.[1] This baffling phenomenon has since then been observed in various liquid crystals ranging from banana-shaped[2] to columnar[3] and nematic phases.[4] In solution, similar chiral symmetry-breaking phenomena have been observed in various self-assembling systems. DeRossi et al. reported one of the earliest examples in their investigations on the self-assembly of benzimidocyanines in solution,[5] while more recently symmetry breaking was reported in self-assembling systems driven by π–π interactions.[6,7] Self-assembling porphyrin-based systems have been studied extensively in this respect, usually when exposed to some kind of external stimulus.[7] Recently, control of handedness of helical aggregates of achiral porphyrin derivatives by applying a combination of rotational and magnetic forces during the self-assembly process gave detailed insights in the underlying mechanisms.[7c] All of these experiments may help in answering one of the most important questions still lingering in science: why do homochiral compounds (L-amino acids and D-sugars) prevail in nature?[8]

Some of these answers may be provided by the interesting observations made in several synthetic, self-assembling systems in which a tiny amount of optically active material suffices to induce a nonproportional response in the optical activity of racemic or achiral systems. This supramolecular analogue of chiral amplification occurs in several helically self-assembling supramolecular polymers and relies on a subtle interplay of different types of noncovalent interactions.[9] Typically, these chiral amplification effects are studied for systems that are in thermodynamic equilibrium and the excess of one enantiomer determines the supramolecular chirality of the system. Benzene-1,3,5-tricarboxamides (BTAs) comprising aliphatic side chains show thermodynamically controlled self-assembly and one-dimensional helical aggregates are formed in a cooperative fashion because of hydrogen bonding.[10] The role of solvent, temperature, concentration, and the position of the methyl substituent in the alkyl side chain of BTAs on the self-assembly process has been elucidated through extensive experimental and theoretical studies.[11]

Symmetry breaking is never observed in homogeneous systems that are racemic or achiral and under thermodynamic equilibrium. When symmetry breaking in achiral molecules is observed, the system is often not under thermodynamic equilibrium. For example, Lehn and co-workers showed a nonstatistical formation of helical handedness in the self-assembly of foldamers,[6b] and in crystallization experiments of amino acid derivatives a nonrandom distribution of the final handedness was observed.[12] In these examples, the systems display secondary nucleation phenomena—that is, part of a preformed crystal or mother fiber initiates the growth of another—in combination with an undetectable amount of chiral impurity.[6b,12]

Here, we report on a class of achiral, partially fluorinated benzene-1,3,5-tricarboxamides (BTAs, Figure 1 class A) that show a unique, two-step self-assembly behavior. After self-assembly into equal amounts of one-dimensional left- (*M*) and right-handed (*P*) helical aggregates that do not show any optical activity under thermodynamic equilibrium conditions, a kinetically controlled secondary nucleation takes place in which the one-dimensional helical aggregates bundle into a higher order aggregate, or fiber, which is optically active. Here we use the term secondary nucleation similar as is used in amyloid aggregation literature, where it describes the thickening of fibrils nucleated at the surface of the first-formed one-dimensional stack to form a fiber.[13] This report is the first on symmetry-breaking in a two-step self-assembling system that relies on a hierarchical self-assembly process in which hydrogen bonding dominates the formation of the helical aggregates and dipole–dipole interactions dominate the secondary nucleation with undetectable amounts of chiral impurities. The first observation of this symmetry breaking was by serendipity, but followed by an in-depth analysis of this discovery with a series of molecules.

[*]   P. J. M. Stals, P. A. Korevaar, M. A. J. Gillissen, Dr. T. F. A. de Greef,
      Dr. C. F. C. Fitié, Prof. Dr. R. P. Sijbesma, Dr. A. R. A. Palmans,
      Prof. Dr. E. W. Meijer
      Institute for Complex Molecular Systems and
      Laboratory of Macromolecular and Organic Chemistry
      Eindhoven University of Technology
      P. O. Box 513, 5600 MB Eindhoven (The Netherlands)
      E-mail: r.p.sijbesma@tue.nl
              a.palmans@tue.nl
              e.w.meijer@tue.nl

Supporting information for this article, including detailed experimental information, that is, synthetic procedures, equipment used, and details on sample preparation, is available on the WWW under http://dx.doi.org/10.1002/anie.201204727.
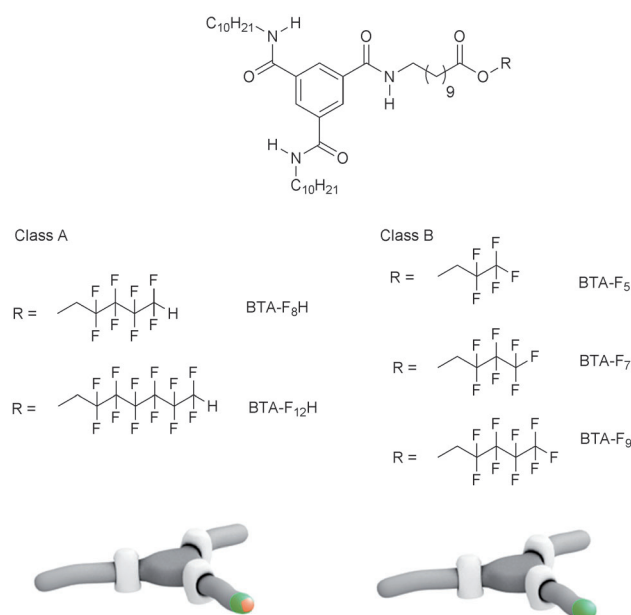
Figure 1. Chemical structures of the partially fluorinated BTAs and their schematic representation (the green part represents the fluorinated part, while the orange part represents the ω-proton).

BTAs comprising two *n*-decyl chains and one partially fluorinated chain (BTA-F$_5$ to BTA-F$_{12}$H, Figure 1) were readily prepared by a multistep synthesis (see Scheme S1 in the Supporting Information). Two types of partially fluorinated chains were employed, resulting in two classes of fluorinated BTAs. In class A a hydrogen atom is present on the ω-position of the fluorinated chain. Two derivatives of this class, differing in length of the fluorinated part were prepared (BTA-F$_8$H and BTA-F$_{12}$H). The ω-hydrogen atom is electron-deficient as evidenced by the ^{1}H NMR spectrum of BTA-F$_8$H (Figure S1). Three derivatives were prepared in class B, in which the fluorinated chains lack the electron-deficient hydrogen atom (BTA-F$_5$, BTA-F$_7$, and BTA-F$_9$). The purity of all BTA compounds was confirmed by ^{1}H, ^{13}C, ^{19}F NMR spectroscopies, elemental analysis, and MALDI-TOF-MS (see the Supporting Information for details). To exclude the possibility that undetectable, non-racemic impurities originating from the starting materials influence the self-assembly process, we synthesized BTA-F$_8$H in four different batches using different starting materials.

The self-assembly of the BTAs was investigated using temperature-dependent circular dichroism (CD) and ultraviolet (UV) spectroscopy in methylcyclohexane (MCH, $c = 3 \times 10^{-5}$ M). The temperature was decreased from 90 to 5°C at a constant rate (60 K h^{-1}) and the CD and UV intensity was monitored at $\lambda = 223$ nm, the maximum of the Cotton effect usually observed for alkyl-substituted carbonyl-centered BTAs.[10c,11a] The temperature-dependent UV curves for the compounds in class B (as example, BTA-F$_9$, Figure 2A) are typical for a cooperative aggregation process involving primary nucleation in

which two regimes can be distinguished: a nucleation regime in which all molecules are molecularly dissolved (indicated by a constant UV signal) and an elongation regime in which the aggregate rapidly grows (indicated by a decrease in UV signal, corresponding to a blue-shift of the UV absorbance of the aggregating BTAs).[10c] The two regimes are separated by the (concentration-dependent) elongation temperature, T_e. For BTA-F$_9$, at a concentration of 3×10^{-5} M, elongation occurs at 334.8 K. As expected, no CD effect was observed for the achiral compounds in class B, since self-assembly results in equal amounts of *P* and *M* helical one-dimensional aggregates.

The self-assembly of the partially fluorinated BTAs in class A (for example, BTA-F$_8$H, Figure 2B, full spectra shown in Figure S2) is quite different from those of class B. In addition to the characteristic transition that we ascribe to the primary nucleation of one-dimensional helical aggregates, there is a second transition, as observed by UV/Vis spectroscopy, around room temperature. Intriguingly, this transition coincides with the unexpected appearance of a CD effect, indicative of a second transition into an optically active fiber. This behavior was found for all batches of BTA-F$_8$H, prepared from different starting materials, and for BTA-F$_{12}$H (Figure S3). Linear dichroism, linear birefringence, precipitation or other known artefacts were all excluded as sources for the observed CD effect.[14]

Surprisingly, the shape of the Cotton effect measured for BTA-F$_8$H and BTA-F$_{12}$H (Figure 2C) differs significantly from that of previously observed alkyl-substituted BTAs, in which either a single maximum at $\lambda = 223$ nm or a maximum peak at 216 nm and a shoulder at 242 nm were observed.[11a,c] For BTA-F$_8$H and BTA-F$_{12}$H the maximum is significantly red-shifted to around 253 nm. Also, the molar ellipticity, $\Delta\varepsilon$,
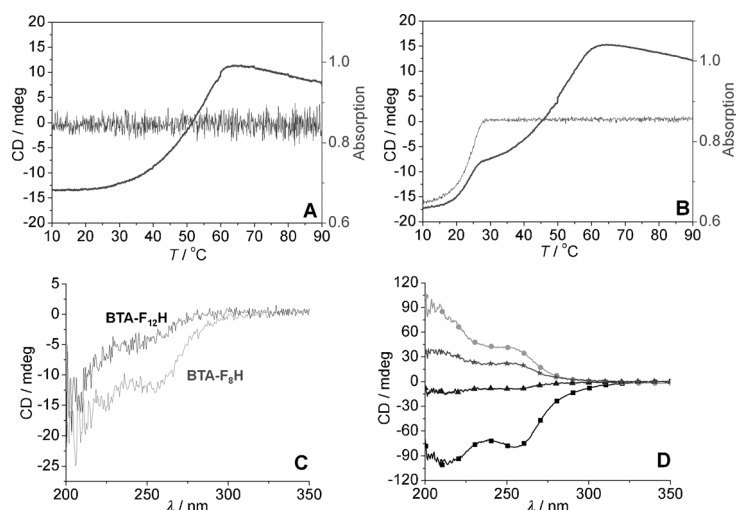

Figure 2. Temperature-dependent UV (black) and CD measurements (gray) of A) BTA-F$_9$ and B) BTA-F$_8$H ($c = 30$ μM in MCH, probed at $\lambda = 223$ nm, $l = 1$ cm). C) CD effects for BTA-F$_8$H (light gray) and BTA-F$_{12}$H (dark gray; $c = 30$ μM in MCH, $l = 1$ cm, $T = 293$ K). D) CD effects observed for BTA-F$_8$H in the absence of additives (dark-gray triangle; normally observed negative CD effect and gray star; rarely observed positive CD effect) and after the addition of S-pyroglutamic acid (positive CD effect, light-gray circle) or of D-tartaric acid (negative CD effect, black square).

(BTA-F$_8$H: $\Delta\varepsilon = -10.1$ L mol^{-1} cm^{-1} at 20°C and BTA-F$_{12}$H: $\Delta\varepsilon = -7.0$ L mol^{-1} cm^{-1} at 20°C) is substantially lower than that of enantiomerically pure BTAs ($|\Delta\varepsilon| = 40$ L mol^{-1} cm^{-1}).[10c,11a,c] Although the temperature-dependent UV and CD cooling curves for BTA-F$_{12}$H and BTA-F$_8$H show similar features (Figure 2 B and Figure S3), the second transition temperature (T_t) for BTA-F$_{12}$H is higher than that for BTA-F$_8$H (310 and 299 K, respectively). The lower $|\Delta\varepsilon|$ found for BTA-F$_{12}$H in combination with a higher T_t indicates that the longer fluorinated part results in a higher-order aggregate or fiber that has a less pronounced preference between the two possible forms than BTA-F$_8$H but is more readily formed.

The formation of optically active fibers from achiral BTA-F$_8$H and BTA-F$_{12}$H is not limited to MCH as solvent, but is also observed in other cyclic alkanes (cyclohexane and decaline, see Figure S4). In linear alkanes (e.g. heptane and dodecane), BTA-F$_8$H and BTA-F$_{12}$H were poorly soluble, while they are molecularly dissolved in more polar solvents such as chloroform.

In general, the CD effects for BTA-F$_8$H and BTA-F$_{12}$H (Figure 2 D, black curve) show a negative sign. In rare cases, however, also positive CD effects were observed for BTA-F$_8$H (Figure 2 D, dark-gray curve). This is a remarkable observation since a stochastic process in the absence of chiral information should result in an equal occurrence of positive and negative CD effects. Noorduin et al. recently reported enantiomerically enriched crystals obtained by abrasive grinding and solution racemization. Deviations from a statistical distribution of enriched crystals were attributed to minute, enantiomerically enriched impurities.[12,15] Hence, we investigated the effect of adding small amounts of insoluble, chiral additives to 30 μM solutions of BTA-F$_8$H in MCH. After heating and cooling these solutions, the addition of, for example, *S*-pyroglutamic acid resulted in a larger, positive CD effect (Figure 2 D), whereas addition of *S*-(−)-phenylglycine, D-tartaric acid or L-tartaric acid resulted in negative CD effects (Figure 2 D). Similar effects were observed for BTA-F$_{12}$H (Figure S5). These results suggest that surface-assisted secondary nucleation may play a role in the formation of the optically active fibers and that minute chiral impurities present in the environment influence the sign and magnitude of the observed CD effect.

We further investigated the fibers formed by BTA-F$_8$H with atomic force microscopy (AFM) and dynamic light scattering (DLS) measurements. Solutions of BTA-F$_8$H in dichloroethane (0.8 mg mL^{-1}) were placed in a chamber filled with MCH. After five days, 5 μL of this solution was dropcasted on mica, allowed to dry and subsequently measured with AFM. Figure 3 A shows a representative amplitude image of the resulting fibers. Fibers with a diameter of 60 nm were observed, significantly larger than the diameter of a one-dimensional BTA aggregate, which would have a diameter of approximately 1.6 nm.[11a] DLS measurements conducted on

solutions of BTA-F$_8$H at a concentration of 30 μM in MCH showed the appearance of large aggregates below 30°C with a hydrodynamic radius (R_H) of about 50 nm (Figure S6).[16] The combined AFM and DLS results suggest that the optically active aggregates have a larger diameter than that of the one-dimensional BTA aggregates, implying that they are formed by bundling of one-dimensional BTA aggregates.

The differences in self-assembly observed between the BTAs of classes A and B indicate that the electron-deficient hydrogen at the ω-position of the partially fluorinated chain is essential for the formation of optically active bundles. The different behavior of -CF$_2$-H and -CF$_3$ end groups in the hierarchical self-assembly is rationalized by the high polarization of the C−F bond.[17] This causes polarization of the C−H bond on the same carbon resulting in the formation of CF$_2$−H···F−CFH interactions between two or more BTA stacks. Although the interaction between an electron-deficient hydrogen and fluorine is weak,[18] C−H···F interactions are stabilizing as shown by several examples in supramolecular chemistry and crystal engineering.[19] However, because of the weak character of these fluorine–hydrogen interactions, multiple interactions are required to bundle one-dimensional BTA aggregates. Previously, we showed that small energy differences between left- and right-handed helicity in one-dimensional helical BTA aggregates can be amplified by the cooperative character of the self-assembly process.[20] Hence, we propose that—prior to bundling—the fluorinated chains at the periphery of a one-dimensional helical BTA aggregate form a ribbon, resulting in a fluorine-enriched patch on the periphery of the one-dimensional aggregates (Figure 3 D). As a result of this one-dimensional microphase separation, the fluorine-enriched ribbons facilitate the hierarchical bundling or surface-assisted secondary nucleation of one-dimensional aggregates into optically active fibers.
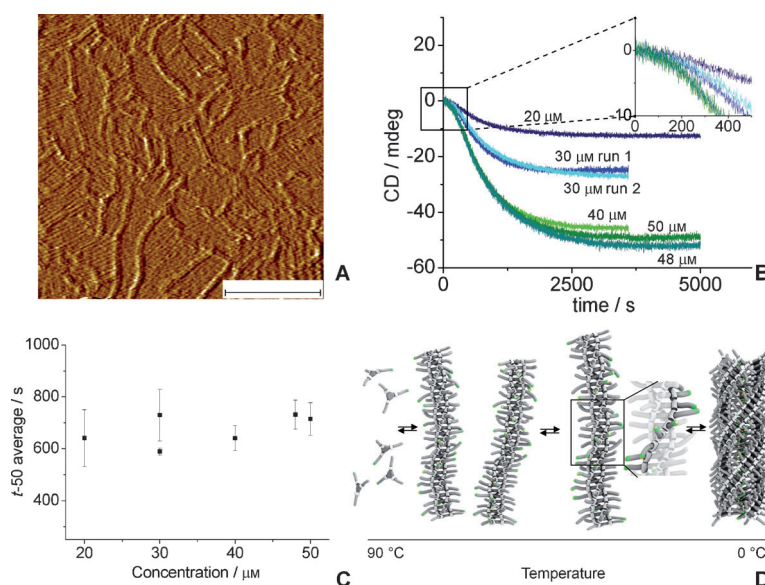

Figure 3. Panel A: AFM amplitude micrograph for dropcasted solutions of BTA-F$_8$H on mica (scale bar = 0.5 μm). Panels B and C: Results of stopped-flow experiments for solutions of BTA-F$_8$H. Panel D: Proposed self-assembly mechanism for partially fluorinated BTAs of class A.

To unravel the mechanism involved in the formation of the optically active bundles for BTA-F$_8$H, we studied the temperature-dependent aggregation using a combination of UV/Vis and CD spectroscopy at different concentrations. The sharp transitions observed in the UV/Vis absorption at 223 nm at the elongation temperature (T_e) and in the CD effect at the critical bundling temperature (T_t) reveal that nucleation phenomena are involved both in the formation of the optically silent one-dimensional aggregates as well as in the subsequent bundling into optically active fibers (Figure S7).[21] The temperature T_e as derived from UV/Vis spectroscopy follows a concentration dependence in agreement with the nucleated formation of one-dimensional helical aggregates: the Van't Hoff plot (logarithm of concentration vs. $1/T_e$, Figure S8) results in an enthalpy of elongation (ΔH_e) of -63 kJ mol^{-1}, which is close to previously reported values for nonfluorinated BTA systems.[10c, 11a,c] Whereas the temperature-dependent assembly of one-dimensional helical aggregates occurs under thermodynamic control,[10c] significant hysteresis was observed in the formation and disappearance of the CD effect upon subsequent cooling and heating (Figure S9). The slow dynamics in the formation of the optically active fibers is in sharp contrast to the formation of one-dimensional aggregates consisting of BTAs substituted with aliphatic side-chains in which case the self-assembly is close to being diffusion-controlled and hence is practically always under thermodynamic control.[10c]

The slow dynamics in the formation of the optically active BTA-F$_8$H fibers prompted us to study the aggregation kinetics in detail using stopped-flow CD spectroscopy. The kinetic profiles were obtained by injection of a solution of BTA-F$_8$H from dichloroethane (a good solvent) into an excess of MCH, thereby initiating the hierarchical self-assembly of BTA-F$_8$H. The subsequent formation of optically active bundles was probed by following the CD effect at $\lambda = 223$ nm as a function of time at 10 °C and at concentrations of 20, 30, 40, 48, and 50 μM (Figure 3 B and Figure S11). A lag phase was observed in the initial stages of the aggregation process, as expected for nucleated aggregation.[22] However, in contrast to kinetic studies on the aggregation of porphyrin, oligo-(p-phenylene vinylene) derivatives, and proteins,[23] both the lag phase as well as the time at which the conversion equalled 50 % (t-50) was concentration independent (Figure 3 C). This t-50 concentration independence excludes a mechanism whereby formation of optically active bundles occurs through a homogeneously nucleated mechanism. However, the rate limiting step in the appearance of optically active bundles might be the formation of fluorine ribbons along the periphery of one-dimensional helical BTA aggregates, or the conversion from a racemic mixture of P and M one-dimensional aggregates within the optically active fibers to a nonracemic ratio between P and M one-dimensional aggregates. Alternatively, formation of optically active fibers can occur by surface-assisted secondary nucleation of free monomers along the fluorine ribbon of a one-dimensional BTA aggregate, resulting in a concentration-independent t-50 value as well. For a full analysis of all considered mechanisms, the reader is referred to the Supporting Information.

The results clearly indicate that the formation of optically active fibers of fluorinated BTA moieties comprises two steps: 1) the cooperative, hydrogen-bond-driven aggregation into one-dimensional helical aggregates consisting of equal amounts of P and M helices under thermodynamic control, and 2) the formation of optically active fibers with a fluorinated core in which one of the two helical one-dimensional aggregates dominates (Figure 3 D). Although we expect a stochastic process in the formation of the optically active fiber, the involvement of chiral impurities results in a preference towards one helicity, even when different compounds and synthetic batches are considered.

Concluding, we have analyzed the symmetry breaking in the self-assembly of a new class of achiral and partially fluorinated BTAs, which show a unique two-step self-assembly. A crucial element in the symmetry breaking is the presence of weak interactions between fluorine atoms and electron-deficient (CF$_2$-H) hydrogen atoms on the periphery of the fluorinated BTA stacks. These fluorine–hydrogen interactions result in bundling of one-dimensional BTA aggregates by secondary nucleation, in which the influence of a minute chiral impurity is strongly amplified. We believe that the observations discussed and rationalized here will provide new insights in understanding serendipitously found symmetry-breaking processes.

[1] W. R. Young, A. Aviram, R. J. Cox, *J. Am. Chem. Soc.* **1972**, *94*, 3976–3981.

[2] T. Niori, T. Sekine, J. Watanabe, T. Furukawa, H. Takezoe, *J. Mater. Chem.* **1996**, *6*, 1231–1233.

[3] H. Nagayama, S. K. Varshney, M. Goto, F. Araoka, K. Ishikawa, V. Prasad, H. Takezoe, *Angew. Chem.* **2010**, *122*, 455–458; *Angew. Chem. Int. Ed.* **2010**, *49*, 445–448.

[4] T. Kajitani, H. Masu, S. Kohmoto, M. Yamamoto, K. Yamaguchi, K. Kishikawa, *J. Am. Chem. Soc.* **2005**, *127*, 1124–1125.

[5] U. De Rossi, S. Dahne, S. C. J. Meskers, H. P. J. M. Dekkers, *Angew. Chem.* **1996**, *108*, 827–830; *Angew. Chem. Int. Ed. Engl.* **1996**, *35*, 760–763.

[6] a) M. Kimura, T. Hatanaka, H. Nomoto, J. Takizawa, T. Fukawa, Y. Tatewaki, H. Shirai, *Chem. Mater.* **2010**, *22*, 5732–5738; b) S. Azeroual, J. Surprenant, T. D. Lazzara, M. Kocun, Y. Tao, L. A. Cuccia, J.-M. Lehn, *Chem. Commun.* **2012**, *48*, 2292–2294.

[7] a) P. Chen, X. Ma, P. Duan, M. Liu, *ChemPhysChem* **2006**, *7*, 2419–2423; b) J. M. Ribó, J. Crusats, F. Sagués, J. Claret, R. Rubires, *Science* **2001**, *292*, 2063–2066; c) N. Micali, H. Engelkamp, P. G. van Rhee, P. C. M. Christianen, L. Monsù Scolaro, J. C. Maan, *Nat. Chem.* **2012**, *4*, 201–207; d) K. Okano, O. Areaga, J. M. Ribo, T. Yamashita, *Chem. Eur. J.* **2011**, *17*, 9288–9292.

[8] a) W. A. Bonner, *Origins Life Evol. Biosphere* **1991**, *21*, 59–111; b) P. L. Luisi in *The Emergence of Life: From Chemical Origins to Synthetic Biology*, Cambridge University Press, Cambridge, **2006**; c) J. E. Hein, D. G. Blackmond, *Acc. Chem. Res.* **2012**, DOI: 10.1021/ar200316n.

[9] a) M. M. Green, N. C. Peterson, T. Sato, A. Teramoto, R. Cook, S. Lifson, *Science* **1995**, *268*, 1860–1866; b) A. R. A. Palmans, E. W. Meijer, *Angew. Chem.* **2007**, *119*, 9106–9126; *Angew. Chem. Int. Ed.* **2007**, *46*, 8948–8968; c) E. Yashima, K. Maeda, H. Iida, Y. Furusho, K. Nagai, *Chem. Rev.* **2009**, *109*, 6102–6211.

[10] a) M. P. Lightfoot, F. S. Mair, R. G. Pritchard, J. E. Warren, *Chem. Commun.* **1999**, 1945–1946; b) I. A. W. Filot, A. R. A. Palmans, P. A. J. Hilbers, R. A. van Santen, E. A. Pidko, T. F. A. de Greef, *J. Phys. Chem. B* **2010**, *114*, 13667–13674; c) M. M. J. Smulders, A. P. H. J. Schenning, E. W. Meijer, *J. Am. Chem. Soc.* **2008**, *130*, 606–611.

[11] a) P. J. M. Stals, M. M. J. Smulders, R. Martín-Rapún, A. R. A. Palmans, E. W. Meijer, *Chem. Eur. J.* **2009**, *15*, 2071–2080; b) M. M. J. Smulders, P. J. M. Stals, T. Mes, T. F. E. Paffen, A. P. H. J. Schenning, A. R. A. Palmans, E. W. Meijer, *J. Am. Chem. Soc.* **2010**, *132*, 620–626; c) Y. Nakano, T. Hirose, P. J. M. Stals, E. W. Meijer, A. R. A. Palmans, *Chem. Sci.* **2012**, *3*, 148–155; d) P. Besenius, G. Portale, P. H. H. Bomans, H. M. Janssen, A. R. A. Palmans, E. W. Meijer, *Proc. Natl. Acad. Sci. USA* **2010**, *107*, 17888–17893; e) A. J. Markvoort, H. M. M. ten Eikelder, P. A. J. Hilbers, T. F. A. de Greef, E. W. Meijer, *Nat. Commun.* **2011**, *2*, 509; f) C. F. C. Fitié, I. Tomatsu, D. Byelov, W. H. de Jeu, R. P. Sijbesma, *Chem. Mater.* **2008**, *20*, 2394–2404; g) T. F. A. de Greef, M. M. L. Nieuwenhuizen, P. J. M. Stals, C. F. C. Fitié, A. R. A. Palmans, R. P. Sijbesma, E. W. Meijer, *Chem. Commun.* **2008**, 4306–4308; h) P. J. M. Stals, J. F. Haveman, R. Martín-Rapún, C. F. C. Fitié, A. R. A. Palmans, E. W. Meijer, *J. Mater. Chem.* **2009**, *19*, 124–130.

[12] a) W. L. Noorduin, H. Meekes, W. J. P. van Enckevort, B. Kaptein, R. M. Kellogg, E. Vlieg, *Angew. Chem.* **2010**, *122*, 2593–2595; *Angew. Chem. Int. Ed.* **2010**, *49*, 2539–2541; b) W. L. Noorduin, T. Izumi, A. Millemaggi, M. Leeman, H. Meekes, W. J. P. van Enckvert, R. M. Kellogg, B. Kaptein, E. Vlieg, D. G. Blackmond, *J. Am. Chem. Soc.* **2008**, *130*, 1158–1159.

[13] We refer to the term secondary nucleation as is common in amyloid aggregation literature; see for example: V. Foderà, F. Librizzi, M. Groenning, M. van de Weert, M. Leone, *J. Phys. Chem. B* **2008**, *112*, 3853–3858.

[14] M. Wolffs, S. J. George, Ž. Tomović, S. C. J. Meskers, A. P. H. J. Schenning, E. W. Meijer, *Angew. Chem.* **2007**, *119*, 8351–8353; *Angew. Chem. Int. Ed.* **2007**, *46*, 8203–8205.

[15] D. B. Amabilino, R. M. Kellogg, *Isr. J. Chem.* **2011**, *51*, 1034–1040.

[16] SAXS measurements at these concentrations under synchrotron irradiation (at the PSI in Villigen, Switzerland) were unsuccessful, presumably because of the low concentrations used.

[17] M. Hird, *Chem. Soc. Rev.* **2007**, *36*, 2070–2095.

[18] a) W. Caminati, S. Melandri, P. Moreschini, P. G. Favero, *Angew. Chem.* **1999**, *111*, 3105–3107; *Angew. Chem. Int. Ed.* **1999**, *38*, 2924–2925; b) W. Caminati, J. C. López, J. L. Alonso, J.-U. Grabow, *Angew. Chem.* **2005**, *117*, 3908–3912; *Angew. Chem. Int. Ed.* **2005**, *44*, 3840–3844.

[19] a) H. Lee, C. B. Knobler, M. F. Hawthorne, *Chem. Commun.* **2000**, 2486–2486; b) E. D'Oria, J. J. Novoa, *CrystEngComm* **2008**, *10*, 423–436.

[20] S. Cantekin, D. W. R. Balkenende, M. M. J. Smulders, A. R. A. Palmans, E. W. Meijer, *Nat. Chem.* **2011**, *3*, 42–46.

[21] a) P. van der Schoot in *Supramolecular Polymers* (Ed.: A. Cifferi), Taylor & Francis, London, **2005**; b) P. Jonkheijm, P. van der Schoot, A. P. H. J. Schenning, E. W. Meijer, *Science* **2006**, *313*, 80–83.

[22] C. Frieden, *Protein Sci.* **2007**, *16*, 2334–2344.

[23] a) R. F. Pasternack, C. Fleming, S. Herring, P. J. Collings, J. dePaula, G. DeCastro, E. J. Gibbs, *Biophys. J.* **2000**, *79*, 550–560; b) P. A. Korevaar, S. J. George, A. J. Markvoort, M. M. J. Smulders, P. A. J. Hilbers, A. P. H. J. Schenning, T. F. A. de Greef, E. W. Meijer, *Nature* **2012**, *481*, 492–496; c) T. P. J. Knowles, C. A. Waudby, G. L. Devlin, S. I. A. Cohen, A. Aguzzi, M. Vendruscolo, E. M. Terentjev, M. E. Welland, C. M. Dobson, *Science* **2009**, *326*, 1533–1537; d) E. T. Powers, D. L. Powers, *Biophys. J.* **2006**, *91*, 122–132.